

7. Gautam, S. K. and Sumathi, S., Dechlorination of DDT, DDE, and DDD in soil (slurry) phase using magnesium/palladium system. *J. Colloid Interface Sci.*, 2006, **304**, 144–151.
8. Gautam, S. K. and Sumathi, S., Complete dechlorination of DDE/DDD using magnesium/palladium system. *Water Environ. Res.*, 2007, **79**, 430–435.
9. Gautam, S. K. and Sumathi, S., Studies on dechlorination of DDT (1,1,1-trichloro-2,2-bis(4-chlorophenyl)ethane) using magnesium/palladium bimetallic system. *J. Hazard. Mater. Ser. B*, 2007, **139**, 146–153.
10. Cane, P. A. and Williams, P. A., The plasmid-coded metabolism of naphthalene and 2-methylnaphthalene in *Pseudomonas* strains: phenotypic changes correlated with structural modification of the plasmid pWW60-1. *J. Gen. Microbiol.*, 1982, **128**, 2281–2290.
11. Hay, A. G. and Focht, D. D., Cometabolism of 1,1-dichlorophenol-2,2-bis(4-chlorophenyl) ethylene by *Pseudomonas acidovorans* M3GY grown on biphenyl. *Appl. Environ. Microbiol.*, 1998, **64**, 2141–2146.
12. Focht, D. D. and Joseph, H., Degradation of 1,1-diphenylethylene by mixed cultures. *Can. J. Microbiol.*, 1974, **20**, 631–635.
13. Focht, D. D. and Alexander, M., Bacterial degradation of diphenylmethane, a DDT model substrate. *Appl. Microbiol.*, 1970, **20**, 608–611.

ACKNOWLEDGEMENTS. We thank the Department of Biotechnology, New Delhi for providing financial support. We also thank RSIC, IIT-Bombay for permission to use their GC-MS facility.

Received 13 December 2007; revised accepted 19 March 2009

Modelling of sPn phases for reliable estimation of focal depths in northeastern India

E. Uma Devi¹, N. Purnachandra Rao^{2,*} and M. Ravi Kumar²

¹Indian National Center for Ocean Information Services, Hyderabad 500 055, India

²National Geophysical Research Institute, Uppal Road, Hyderabad 500 007, India

In North East India, reliable estimation of earthquake focal depths has always been a problem, owing to paucity of permanent regional seismic stations, constraints on good quality data and lack of crustal models in a complex tectonic terrane. The depth estimations by international agencies, mostly based on teleseismic data, vary from very shallow to even 60 km, suggestive of earthquake occurrence in the upper mantle region. However, modelling of sPn phases in earthquake waveforms that are highly sensitive to focal depths indicates that the earthquake locations are probably well within the crustal layer. The current method has the advantage that dt , the travel time difference bet-

ween sPn and Pn, remains constant for a wide range of source-station distances, and hence enables easy identification of the sPn phase, while providing direct and accurate estimate of the focal depth. The approach is also insensitive to location errors and variations in crustal models, a useful feature especially while dealing with sparse data with high location errors. In the present study, earthquakes in the magnitude range 3.0–4.0 recorded by a network of nine broadband stations in NE India have been analysed. Consistent dt values at different stations were observed for each event, enabling precise depth estimation mostly within ± 1 or 2 km. In general, depths of 15–20 km in the Shillong plateau region, >20 km in the Sylhet basin region and shallow <10 km in the eastern Himalayan foothills are confirmed, that correlate well with the local tectonics. Further, we propose that the flat characteristics of the dt curve that begin to change for earthquakes below the Moho, can be a potential tool for discriminating between crustal and sub-crustal earthquakes, as well as for delineation of the Moho using dense regional seismic networks in future.

Keywords: Crustal models, earthquakes, focal depth, reliable estimation, sPn phase.

THE North East Indian region is regarded as one of the most seismically active regions of the world, having experienced two great earthquakes of magnitude >8.5 (the 1897 Shillong earthquake and the 1950 Assam earthquake), more than a dozen earthquakes of magnitude >7.0 and several tens of earthquakes of magnitude >6.0 during the last century (Figure 1). Most of the seismicity is a consequence of the stresses generated by the sustained collision of the Indian and Eurasian plates in the Eastern Himalayas to the north and the India–Burma plate boundary along the Arakan Yoma fold belt to the east. The wedge formed by these active plate boundaries comprises the Shillong plateau, believed to be uplifting even at present¹; the Mikir Hills, and the alluvium-covered Assam valley in the Himalayan foredeep that contains one of the largest Tertiary oil fields of India. The seismicity distribution suggests that several lineaments in the NE Indian region are active, the most prominent being Kopili, that separates the Shillong plateau and Mikir Hills, the Bomdila and Sylhet lineaments².

In the past, paucity of high-quality, permanent seismic networks in NE India together with complex lateral variations in the crustal structure has posed severe constraints on precise hypocentral locations, especially the focal depths of earthquakes. Out of the 43 earthquakes of magnitude >5 reported by ISC in the foredeep, Shillong plateau, Mikir Hills and Eastern Himalayan region during the period 1964–2003, 11 seem to be located in the upper mantle, considering an average Moho depth of 40 km estimated from receiver function studies³. Using broadband waveform modelling, Chen and Molnar⁴ have indicated that earthquakes in the Shillong plateau region occur as

*For correspondence. (e-mail: raonpc@ngri.res.in)

deep as in the upper mantle, suggestive of a cold lithosphere beneath. In view of the above, resolving whether the uppermost mantle is seismogenic or not assumes great importance, since it has implications for the strength of the continental lithosphere, which in turn has a direct bearing on the geodynamics of this unique continent-continent-collision syntaxis zone.

In the present study we have utilized the regional sPn depth phases of earthquakes in NE India using broadband waveforms recorded in the epicentral distance range of 1°–3.5° and obtained precise estimates of focal depths based on the travel-time difference of the sPn and Pn phases, referred as *dt*. We also suggest that the earlier depth estimates reported by global agencies like the USGS and ISC were probably overestimated. Further, we outline a possible approach for resolving crustal and sub-crustal earthquakes, and also for delineation of the Moho in future based on the characteristics of *dt* curves for dense regional networks.

The data used in this study were from a network of nine broadband stations equipped with 24-bit digitizers synchronized with GPS clock, and operated in the NE Indian region by the National Geophysical Research Institute, Hyderabad (Figure 1). Earthquakes of magnitude

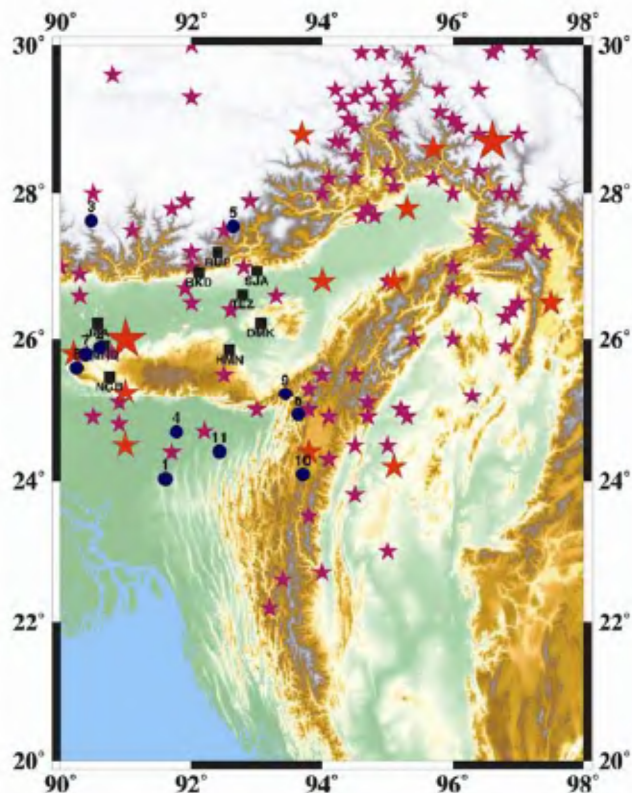


Figure 1. A seismotectonic map of the North East Indian region indicating the earthquakes (circles) and broadband stations (squares) used in the present study. Stars of three different sizes indicate the previous events of magnitude in the range 6.0–7.0, 7.0–8.0 and above 8.0 respectively, in about last 100 years.

>3.5 recorded during 2001–04, and with a good signal-to-noise ratio were analysed in this study (Table 1).

The depth phases like pP and sP reflected at the free surface can be identified and interpreted using broadband data at local to regional distances in order to obtain precise estimates of focal depths. For the *P*-wave, since the energy is much lower than that of the *S*-wave, the pPn phase is generally difficult to identify, as also because it tends to be lost in the *P*-coda. For sPn, the *S*-wave from the source moving upward is reflected back downward as *P* by the free surface with sufficient energy. In the seismic record the Pn phase arrives first followed by the sPn phase which is best visible around a frequency of 1 Hz for regional events. The ray paths of sPn and Pn are shown in Figure 2, when the hypocentre is in the first or the second layer of the crust respectively. To calculate their travel times, let α_1 , β_1 and H_1 be the *P*-wave velocity, *S*-wave velocity and thickness of the first layer respectively, and α_2 , β_2 and H_2 be those of the second layer respectively, and α_3 and β_3 be the *P*- and *S*-wave velocities of the sub-crustal layer. Using ray theory, the time difference between the sPn and Pn phases was obtained as⁵:

$$dt = h \left[\sqrt{\{1/\beta_1^2 - 1/\alpha_3^2\}} + \sqrt{\{1/\alpha_1^2 - 1/\alpha_3^2\}} \right] = h(\eta_{\beta_1} + \eta_{\alpha_1}), \tag{1}$$

where the hypocentre lies in the first layer and *h* is the depth of the hypocentre below the free surface, η_{α_i} and η_{β_i} are the vertical slowness of the *P*- and *S*-waves respectively in the *i*th layer with ray parameter = $1/\alpha_3$. If the hypocentre is in the second layer, then

$$dt = H_1[\eta_{\beta_1} + \eta_{\alpha_1}] + h[\eta_{\beta_2} + \eta_{\alpha_2}], \tag{2}$$

where *h* is the depth below the interface between the first and second layers and H_1 is the thickness of the first layer (Figure 2).

It may be seen from eqs (1) and (2) that the time difference *dt* between the two phases is independent of the epicentral distance.

In the present study several earthquakes recorded during 2001–04 in NE India were analysed, of which 11 events in the delta range 1°–3.5° having clear sPn phases were considered. Each event has at least three stations, and a maximum of five stations clearly recording the sPn phase. Figure 3 shows a few examples where the Pn, Sn and sPn phases have been well identified in the vertical component. The alignment of the sPn phases parallel to the trend of the onset of the Pn phases enables a much easier identification, and is in fact, a good characteristic of this phase, since independence with station delta is unique to sPn. Some scatter can be seen in the alignment of sPn, which can possibly be attributed to local and azimuthal variations in the crustal structure. The mean and

Table 1. A list of earthquakes in the North East Indian region used in the present study, indicating the locations, magnitudes, dt and focal depths from USGS, ISC and the present study along with the error limits. ST, Sylhet Traps; SP, Shillong Plateau; EH, Eastern Himalayas and BA, Burmese Arc

Sl. no	Date YY MM DD	Latitude, °N	Longitude, °E	dt (s)	Depth (km) from USGS	Depth (km) from ISC	Depth (km) present study	Region
1	2001 04 18	24.03	91.60	8.5	10	13.4	23 ± 1.2	ST
2	2001 04 20	25.88	90.60	5.9	33	36.6	15 ± 1.8	SP
3	2001 05 03	27.63	90.47	4.3	33	59.8	11 ± 0.4	EH
4	2002 10 14	24.69	91.77	7.5	33	31.1	20 ± 1.3	ST
5	2002 11 14	27.55	92.64	10.1	61	79.0	27 ± 1.9	EH
6	2003 08 26	24.94	93.64	9.1	45	45.4	24 ± 1.3	BA
7	2003 12 02	25.79	90.39	6.6	23	21.8	17 ± 0.6	SP
8	2003 12 06	25.60	90.25	6.8	26	26.7	18 ± 1.4	SP
9	2004 05 12	25.23	93.44	9.2	57	–	24 ± 0.6	BA
10	2004 11 05	24.09	93.71	10.9	56	–	30 ± 2.7	BA
11	2004 12 07	24.41	92.43	8.3	72	–	22 ± 1.8	ST

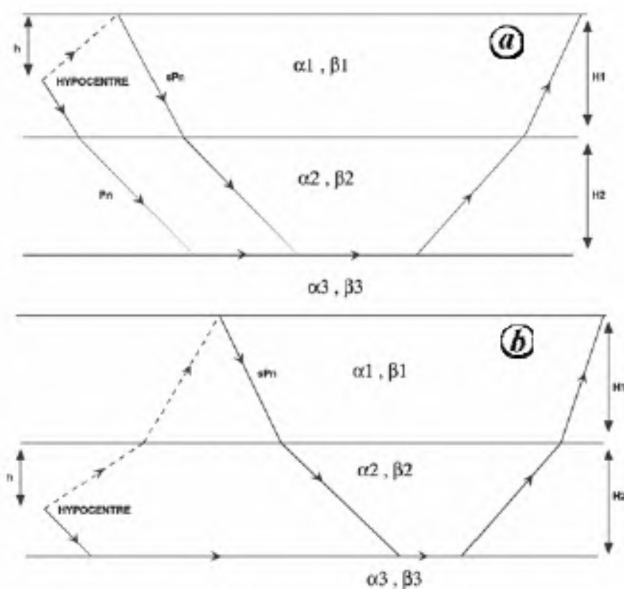


Figure 2. Ray paths for Pn and sPn wave propagation at regional distances for a two-layered crustal model, considered for the cases where the hypocentre is located in (a) the first layer and (b) the second layer (modified after Bhattacharya *et al.*⁵).

standard deviation of this scatter has been estimated for each earthquake, which translates into the focal depth estimate and its error limits respectively, using eqs (1) and (2) and using a simplified version of the crustal model of Gupta *et al.*⁶. In NE India the sedimentary thickness is of the order of only 1 km and preliminary calculations show that the error in focal depth determination is negligible due to the presence of such a sedimentary layer. Table 1 lists the values of focal depths estimated for each of the earthquakes analysed from different terrains of the NE Indian region.

In the western part of the Shillong plateau region (events 2, 7 and 8), focal depths of 15, 17 and 18 km were obtained, indicating shallow upper crustal distribution of

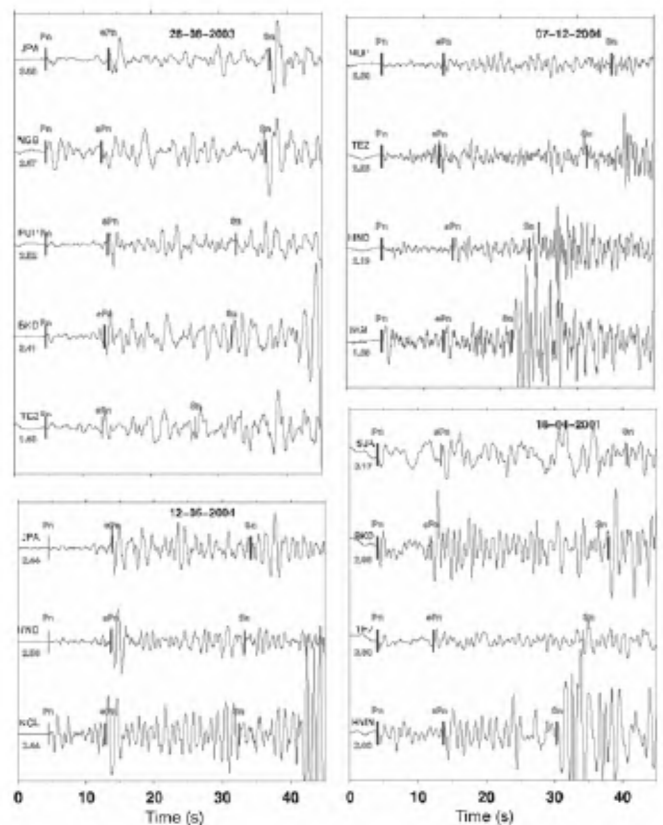


Figure 3. Vertical component broadband seismograms of a few sample events analysed, along with the Pn, Sn and clear sPn depth phases. The waveforms are low-pass filtered and aligned with respect to the Pn arrival times.

focal depths. Earlier, waveform synthesis of long-period body waves recorded by ten stations, but at teleseismic distances yielded focal depths >40 km for two earthquakes in the Shillong plateau region⁴ based on which an especially cold lithosphere was inferred.

In the Sylhet basin region (events 1, 4 and 11), focal depths of 23, 20 and 22 km respectively were indicated. In the Eastern Himalayas (event 3), a shallow focus of

11 km was observed, typical of this region, considering the shallow-dipping decollement plane in the region⁷. Another event in the Eastern Himalayan syntaxis (event 5) indicated a focal depth of 27 km. This is in accordance with the Moho trend inferred in this region by Ramesh *et al.*⁸, using the *P*-to-*S* receiver function technique, where a Moho depth of about 35 km was inferred beneath the Shillong plateau, which increases to 50 km towards Tibet in the north. Events in the Burmese Arc (events 6, 9 and 10) were in the range 24–30 km, although this region is known to have deeper events corresponding to the subducted Indian slab in the east. Importantly, all the events analysed yielded shallow focal depth confined to the crust. A comparison with the estimates from global agencies indicated great discrepancies in the focal depths, with the USGS and ISC estimates reaching down to even 60 km (Table 1). Since the depth estimates based on sPn arrival times, if identified correctly, tend to be accurate even in the case of less accurate epicentral locations or crustal models, it appears that focal depths were probably overestimated in the past.

Table 2. Simplified two-layered velocity model from Gupta *et al.*⁶ used to compute travel times in the present study

<i>P</i> -wave velocity (α) (km/s)	Depth of top of the layer (km)
6.0	0.0
6.7	25.0
8.1	45.0

S-Wave velocity (β) is obtained from $\alpha/\beta = 1.70$.

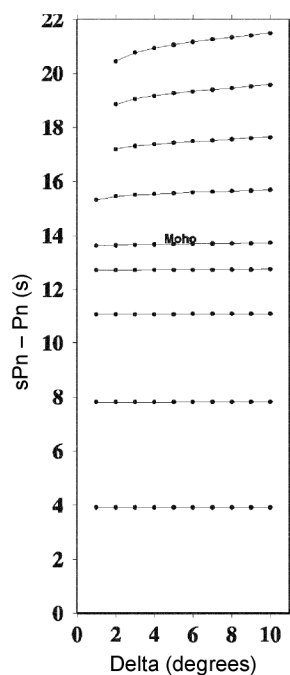


Figure 4. Variation of dt , the theoretical travel-time difference between sPn and Pn, as a function of delta at regional distances (1° – 10°) for all the events listed in Table 1. Note the change in shape of the curves corresponding to focal depths below the Moho.

To understand the constraints on focal depth estimates provided by the sPn phase, we estimated theoretical dt curves as a function of delta for different sets of focal depths, considering a simplified version of the crustal model of Gupta *et al.*⁶ (Table 2). The constancy of dt with respect to delta for each focal depth is clearly depicted in Figure 4, which is in fact an important diagnostic that enables the easy picking of this phase. This flat curve characteristic, however, changes at the Moho crossover level, providing yet another useful diagnostic for identifying a sub-Moho event. It would be interesting to investigate whether this feature of the sPn phase can be useful in future as a constraint for identification of the Moho using data from dense regional networks, where sub-crustal earthquakes occur. Further, it has been demonstrated that variation in crustal models has a minimal effect on dt and hence on focal depths⁹, since most of the travel-time variations get nullified when travel-time differences are considered.

The present study exploits the utility of modelling the sPn phases for reliable estimation of focal depths of regional earthquakes. The sensitivity of the sPn phase to focal depth, and its insensitivity to epicentral errors and variations in crustal models indicate the wide potential of its application. From the present study, it appears, in general, that focal depths in the NE Indian region are mostly confined to the crust and were probably overestimated by global agencies in the past, although detailed modelling of larger data sets would be required to confirm this in future. The characteristic curves of delta vs dt indicate the potential of this approach for resolving crustal and sub-crustal events, and delineation of the Moho in future for a dense regional network with a wide range of earthquake focal depths. Interestingly, application of the sPn phase requires wide delta coverage rather than an azimuthal coverage, suggesting the utility of linear seismic arrays in accurate estimation of focal depths. Since this method is applicable only for regional distances where smaller earthquakes of magnitudes less than 3.0 would not be well recorded, it is suggested that analysis of local depth phases like the sPg would greatly complement the sPn approach for reliable focal-depth estimations at more local distances.

1. Rao, N. P. and Kumar, M. R., Uplift and tectonics of the Shillong plateau, northeast India. *J. Phys. Earth*, 1997, **45**, 167–176.
2. Mukhopadhyay, M., Seismotectonics of transverse lineaments in the eastern Himalaya and its foredeep. *Tectonophysics*, 1984, **109**, 227–240.
3. Kumar, M. R., Raju, P. S., Devi, E. U., Saul, J. and Ramesh, D. S., Crustal structure variations in northeast India from converted phases. *Geophys. Res. Lett.*, 2004, **31**, L17605.
4. Chen, W. P. and Molnar, P., Source parameters of earthquakes and intraplate deformation beneath the Shillong Plateau and the Northern Indoburman ranges. *J. Geophys. Res.*, 1990, **95**, 12527–12552.
5. Bhattacharya, S. N., Ghose, A. K., Suresh, G., Baidya, P. R. and Saxena, R. C., Source parameters of Jabalpur earthquake of 22 May 1997. *Curr. Sci.*, 1997, **73**, 855–863.

6. Gupta, H. K., Singh, S. C., Dutta, T. K. and Saikia, M. M., Recent investigations of northeast India seismicity. In Proc. Int. Symp. Continental seismicity and earthquake prediction. Seismological Press, Beijing, 1984, pp. 63–71.
7. Ni, J. and Barazangi, M., Seismotectonics of the Himalayan collision zone: geometry of the underthrusting Indian plate beneath the Himalaya. *J. Geophys. Res.*, 1984, **89**, 1147–1163.
8. Ramesh, D. S., Kumar, M. R., Devi, E. U., Raju, P. S. and Yuan, X., Moho geometry and upper mantle images of North-East India. *Geophys. Res. Lett.*, 2005, **32**, L14301.
9. Barbano, M. S., Kind, R. and Zonno, G., Focal parameters of some Friuli earthquakes (1976–1979) using complete theoretical seismograms. *J. Geophys.*, 1985, **58**, 175–182.

ACKNOWLEDGEMENTS. We are grateful to Dr V. P. Dimri, Director, NGRI, Hyderabad for constant support and encouragement. This work was carried out under a project sponsored by the Department of Science and Technology, New Delhi. E.U.D. is grateful to the Council of Scientific and Industrial Research, New Delhi for the senior research fellowship.

Received 8 August 2007; revised accepted 2 March 2009

Variations in snow cover and snowline altitude in Baspa Basin

Rakesh Kaur^{1,*}, D. Saikumar¹, Anil V. Kulkarni² and B. S. Chaudhary³

¹National Technical Research Organisation, New Delhi 110 067, India

²Space Applications Centre, Ahmedabad 380 015, India

³Kurukshetra University, Kurukshetra 136 118, India

The Himalayas has one of the largest concentrations of glaciers and permanent snowfields outside the polar region. Snow and glacier melt forms an important source for many rivers originating in the Himalayas. Numerous studies suggest that global warming has started affecting snow melt and stream run-off in the Himalayan region. Monitoring the snow-cover changes is therefore essential to assess the future hydrologic cycle. Snowline altitude is an important parameter to assess future changes in snow cover. Variations in snowline altitude and snow cover for the years 2004–05 and 2006–07 between October and June for Baspa River Basin located in the Kinnaur District, Himachal Pradesh are reported here. The snow cover was delineated using 54 images of AWiFS sensor of Resourcesat-I satellite using NDSI technique and elevation information was generated using SRTM data. About 98% of the basin area is located below the elevation of 5800 m. The average monthly snowline altitude was estimated. The lowest snowline altitude was

observed as 2425 m in February 2004–05 and 2846.25 m in March in 2006–07.

Keywords: Baspa Basin, global warming, snow cover, snowline.

THE Himalayas is one of the youngest mountains in the world and accounts for almost 70% of non-polar glaciers. The Himalayan region has permanent snow fields and in winter most of the high-altitude regions experience snowfall¹. During summer, snow melt is the major run-off for many rivers originating from the Himalayas, the lifeline of millions of people. Therefore, monitoring the changes in snow-cover area is essential not only for the development of ecosystems, but also for human activities like agriculture, hydropower generation, etc. Snow cover is highly dynamic and has a great influence on the local climate due to high albedo.

During the 20th century, the rapid industrialization caused a huge increase in global temperature by changing the composition of the atmosphere with large emissions of CO₂, other trace gases and aerosols². By 2100, the global surface temperature is projected² to increase by 1.4–5.8°C. The Intergovernmental Panel on Climate Change (IPCC) has estimated that with increasing level of global warming, regions receiving snowfall will increasingly receive precipitation in the form of rain and for every 1°C increase in temperature³, the snowline will rise by about 150 m.

The snowline is a line that divides the snow-cover surface and the barren surface at a given point of time⁴. The snowline is an important indicator of snow coverage and when viewed over a large area, the elevation shift of the snowline indicates a certain climate behaviour, either to a cold or a warm climate. A periodical study of the spatial-temporal variations of the snowline can help in assessing the hydrologic cycle balance as well as to understand the regional and global climatic changes.

The Baspa River Basin, a major tributary of the Satluj river, is located in Kinnaur District, Himachal Pradesh.

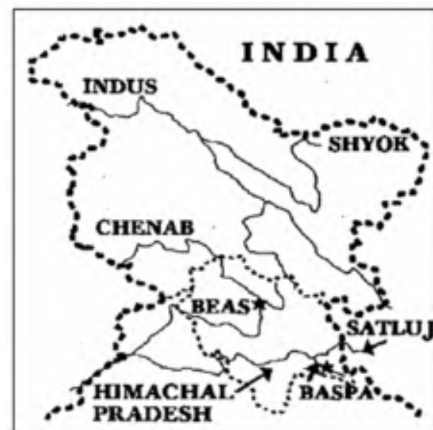


Figure 1. Location map of Baspa Basin, Himachal Pradesh, India.

*For correspondence. (e-mail: rkaur.rana@gmail.com)